Catalytic effects of shale ash with different particle sizes on characteristics of gas evolution from retorting oil shale

Xiang Ge[1] · Sha Wang[1] · Xiumin Jiang[2]

Abstract

Huadian oil shale samples were pyrolyzed in a small retort at 520 °C in the absence and presence of shale ashes with different particle sizes of 0–0.20 mm, 0–0.60 mm and 0–1.25 mm under argon atmosphere to evaluate the catalytic effects of shale ash on the products yield and non-condensable gases evolution characteristics. The shale ash samples were recorded as 0.20 mm, 0.60 mm and 1.25 mm shale ashes. The results indicate that the shale ash samples with good adsorption capacity and certain catalytic performance significantly affect the reactivity of oil shale pyrolysis. There are a slight decrease in the shale char yield and an increase in the total yield of volatile products with the particle size of shale ash decreasing from 1.25 to 0.20 mm. The shale oil yield increases after adding 0.20 mm and 0.60 mm shale ashes, especially 0.20 mm, but decreases after adding 1.25 mm shale ash compared with that obtained without adding shale ash, while the non-condensable gases yield decreases after adding shale ashes with three particle sizes, especially 0.60 mm. In addition, the gas products contain higher-volume content of CO_2, CH_4 and H_2, and lower-volume content of CO and C_2–C_4 hydrocarbons. Adding the shale ash makes the peak concentrations of all gases shift to the lower temperatures and increases the maximum peak concentrations of C_4H_8 and H_2, especially H_2, but decreases those of other gases. The non-condensable gases mainly contain CO_2 and CH_4, and smaller amounts of other gases in terms of their mass distribution. The addition of shale ashes reduces the yields of several gases except CO_2, H_2, C_2H_6 and C_4H_8 compared with those obtained without adding shale ash. Adding three shale ash samples increase the H_2 content, but cause different effects on the contents of CO_2, C_2H_6 and C_4H_8. Among three shale ash samples, adding 1.25 mm shale ash produces the largest amount of CO_2 and CO, as well as the lowest total content of C_2–C_4 alkenes, while adding 0.60 mm shale ash produces the largest amount of H_2 and largest total content of C_1–C_4 alkanes. Adding the shale ash decreases the ethene/ethane ratio and increases the other alkene/alkane ratios compared with those obtained without adding shale ash. Adding 0.2 mm shale ash among three shale ash samples produces the lowest ethene/ethane and propene/propane ratios, being possibly related to the most significant coking reactions. Adding shale ashes with smaller particle sizes are more conducive to obtain non-condensable gases of higher heating value. The addition of 0.20 mm shale ash is the optimal for improving the shale oil yield and the conversion rate of kerogen to volatile products.

Keywords Oil shale retorting · Shale ash · Products yield · Non-condensable gases · Characteristics

Introduction

With the continuous increase in energy demand for conventional hydrocarbon reserves, oil shale has been considered as a predominant alternative source for alleviating the pressure of oil and gas supplies. China contains abundant oil shale reserves which are estimated to be 720 billion tons, i.e., 47.6 billion tons of in situ recoverable shale oil, representing potential sources of hydrocarbons [1, 2]. The kerogen in the oil shale can be converted to shale oil and

✉ Sha Wang
  wangsha_84@163.com

1 Institute of Thermal Energy and Power Engineering, College of Mechanical Engineering, Shanghai University of Engineering Science, Shanghai 201620, People's Republic of China

2 Institute of Thermal Energy Engineering, School of Mechanical Engineering, Shanghai Jiao Tong University, Shanghai 200240, People's Republic of China

gases by retorting process, in which there are several physical and chemical reactions occurring simultaneously in series and parallel. The produced gas products have relatively high energy values and therefore can be used as potential fuels [3]. Their yields and characteristics depend on several factors, such as the components of oil shale, primary reactions as well as the experimental conditions (retorting temperature, heating rate, residence time, particle size, retorting atmosphere, catalysts, etc.) and reactor types (fischer assay, fixed bed, fluidized bed, rotary kiln, etc.), which affect the secondary reactions of the primary pyrolysis volatiles [4–9]. For producing gas products with high yield and high qualities, it is necessary to investigate their evolution characteristics under different retorting conditions.

So far, some investigations have mainly focused on the evolution kinetics of the light gases (CO_2, CO, H_2, CH_4 and low molecular weight hydrocarbons) generated during retorting oil shale as well as their content distribution in the absence of catalyst under different temperatures and heating rates [10–14]. As reported by these studies, the alkene to alkane ratios were dependent on the heating rate, pyrolysis temperature, the type of oil shale and to a lesser extent on the degree of conversion, which have been used extensively as indicators of oil shale retorting conditions and might be related to secondary cracking and coking reactions of oil vapors. Furthermore, some sulfur-containing gases have been determined during the non-catalytic pyrolysis of oil shale [15, 16].

On the other hand, a few studies have investigated on the yield distribution of gas products released during the catalytic pyrolysis of oil shale. The catalysts commonly used in the catalytic pyrolysis of oil shale mainly included alkali metals, alkaline earth metals and transition metallic species as well as their compounds [9, 17]. Some researchers have demonstrated that alkali and alkaline earth metal cations might affect the reactivity of the oil shale pyrolysis. As reported, the addition of calcium-based catalysts contributed to the cracking of oxygen-containing functional groups during oil shale pyrolysis and could effectively remove CO_2 and gas-phase sulfur-containing compounds [18–21]. Moreover, it was considered that the transition metal iron had high catalytic activity for hydrogenation and dehydrogenation reactions [22, 23]. Hascakir et al. [24] have indicated adding three different iron powders (Fe, Fe_2O_3 and $FeCl_3$) improved the thermal conductivity of the oil shale samples to accomplish efficient temperature distribution. The oil viscosity reduced at higher temperature, which contributed to raise oil recovery from oil shale [25]. And Fe_2O_3 showed positive effect on the breakdown of organic fuels [26]. In addition, Jiang et al. [27] proposed that the transition metal Co ion also could act as the activation center to accelerate the breakdown of chemical bonds in organic matters of oil shale, and the Co ion could increase the selectivity of aromatic hydrocarbons and promote olefin aromatization. Williams and Chishti [28, 29] developed a two-stage oil shale pyrolysis reactor incorporating a second batch reactor using zeolite ZSM-5 catalyst. The results suggested that the gas products were consisted of mainly CO_2, CO, H_2, CH_4, C_2H_4, C_2H_6, C_3H_6, C_3H_8 and some minor hydrocarbon gases, whose concentrations significantly increased after the catalyzed process.

Moreover, mineral matters present in oil shale were also believed to play important roles in the thermally induced catalytic alternation of kerogen during pyrolysis reactions of oil shale. The shale ash obtained by combusting oil shale also exhibited certain catalytic activity because it contained SiO_2, Al_2O_3, CaO, Fe_2O_3 and other mineral matters. Some studies have investigated the effect of the mineral matrix of oil shale on the conversion of kerogen into organic materials during pyrolysis reactions [30, 31]. Their results suggested that pyrolysis reactions were catalyzed by alkaline earth metal cations in carbonates and inhibited by silicates. The inhibition effect of the silicates seemed to be greater than the catalytic effect of the carbonates on the pyrolysis reactions of the original oil shales [18, 32, 33]. Liu [34] have indicated the shale ash had certain catalysis function in solid heat carrier retorting of oil shale. Shi et al. [35] showed that adding shale ash promoted the decomposition of organic matters and mineral matters [36, 37]. Huang et al. [38] have reported that shale ash had relatively moderate activity for adjusting the secondary reactions of pyrolysis volatiles in the applied range of residence time. Dung [39] has investigated the influence of shale ash on the coking reactions of oil vapors. The yields of gas products except methane and hydrogen were unchanged by the coking reactions. Carter et al. [40, 41] also have presented that the shale ash had the greatest influence on the coking reaction of oil vapors compared with shale char and gasified shale, especially certain types of clay minerals in the shale ash [42]. After adding shale ash, there were a significant decrease in the average molecular weight and an increase in the aromaticity of the shale oil [40, 41]. However, it is still rarely reported the evolution properties of gas products with time in the catalytic pyrolysis process of oil shale using the shale ash as the catalyst, and the catalytic mechanism of the shale ash during the pyrolysis of oil shale.

In this paper, oil shale samples obtained from Dachengzi mine located in Huadian city of China were retorted in a stainless retort at 520 °C under argon atmosphere in the absence and presence of shale ash to investigate the effect of the shale ashes with different particle sizes on the products yield and evolution properties of gas products. The gases produced were characterized using a multi-

component Fourier transform infrared (FTIR) gas analyzer GASMET DX-4000 for determining major non-hydrocarbon gases (CO and CO_2), C_1–C_4 hydrocarbons gases concentrations and an MRU-Vario Plus industrial portable flue gas analyzer for determining H_2 and CO_2 concentrations. Such information is needed not only to understand the pyrolysis reaction mechanism, but also to optimize the pyrolysis conditions and promote the pyrolysis of oil shale.

Experimental

Raw material and catalysts

Oil shale samples investigated in this paper were obtained from Dachengzi mine located in Huadian city, China. The general characteristics of the samples are given in Table 1 [43, 44]. The original oil shale samples were crushed and screened to an average particle size of less than 3 mm according to the National Standards of China (GB 474-1996). All samples were dried at 105 °C to constant mass and then stored in a desiccator. The shale ashes with three particle sizes of 0–0.2 mm, 0–0.6 mm and 0–1.25 mm were, respectively, recorded as 0.2 mm, 0.6 mm and 1.25 mm shale ashes, which were chosen as candidate catalysts based on comprehensive evaluation about their scientific and technical factors besides their economic consideration. They could easily be obtained from the bottom ash produced by a 65 t h^{-1} circulating fluidized bed combustion at 850 °C. During the experiments, all catalysts were mechanically mixed with oil shale and the mass of each shale ash sample was 10% of the oil shale mass.

Experimental setup and procedure

All experiments were performed in a stainless-steel cylindrical retort (70 mm i.d., 100 mm height), as shown in Fig. 1. The temperature of the reactor vessel was measured by a thermocouple and controlled by proportional–integral–derivative (PID) controller [45]. To study the effect of the shale ashes with different particle sizes on products

yield and non-condensable gases evolution characteristics, 50 g of dried oil shale sample and three mixture samples of 50 g of dried oil shale sample and 5 g of shale ash with three particle sizes of 0–0.20 mm, 0–0.60 mm and 0–1.25 mm were, respectively, fed into the reactor electrically heated at a heating rate of 12 °C min^{-1} from room temperature to 520 °C and held for 20 min under argon atmosphere. The volatile products escaped from the reactor have been cooled by a series of cold traps which were immerged in low-temperature troughs (~ 0 °C) filled with the mixture of ice and water. The liquid products have been separated from gases, and then, they were further divided into shale oil and water based on their density differences in another separation unit. Gas products were sampled into the online gas analyzers. The mass of shale char and liquid products was determined, while the non-condensable gases yield was calculated by overall mass balance. In this study, all the experiments were repeated twice and the product yields were calculated by an average value of two equivalent tests.

Shale ash analysis

The nitrogen adsorption–desorption isotherms were measured for shale ash samples at 77.8 K using a Micromeritics ASAP 2010-M + C surface area and porosimetry analyzer. The relative pressure ratio of P/P_0 (P was the equilibrium pressure and P_0 was the saturation pressure) ranged from 0.01 to 0.995, and the pore size ranged from 1.7 to 300 nm. The specific surface area of the samples was calculated using the Brunauer–Emmett–Teller (BET) model. And the pore size distribution was determined by the Barret–Joyner–Halenda (BJH) method using the corresponding desorption branches of the isotherms [46]. The X-ray power diffraction (XRD) analyses of shale ash samples were performed on a Rigaku D/max-2200 X-ray diffractometer using Cu $K\alpha$ radiation source generated at 40 kV and 20 mA, and the diffraction data were recorded by continuous scan in the 2θ range from 5° to 90° with a scan rate of 0.02°/s.

Table 1 Analysis of Dachengzi oil shales (as received basis)

Proximate analysis/mass%		Ultimate analysis/mass%		Retorting assay data[b]/mass%	
M	11.54	C	27.33	Shale oil	19.20
A	48.24	H	3.59	Shale char	63.77
FC	4.02	O[a]	7.89	Water	11.88
VM	36.20	N	0.57	Gases	5.15
Low heating value/kJ kg^{-1}	11,076.07	S	0.84		

[a]Oxygen content was determined by difference

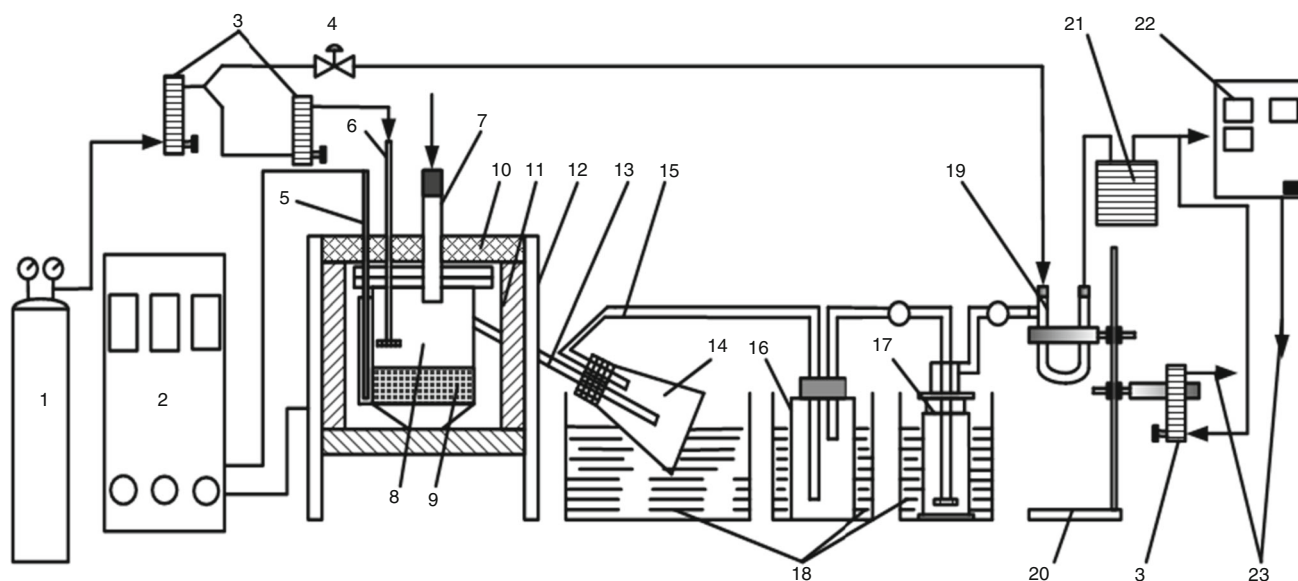[b]Under the national standard of China (SH/T 0508-92)

Fig. 1 Schematic diagram of experimental retorting system of oil shales. 1 argon cylinder, 2 automatic temperature controller, 3 flowmeter, 4 flow control valve, 5 thermocouple, 6 gas inlet, 7 sample inlet, 8 retort reactor, 9 oil shale, 10 insulation, 11 electric heater, 12 steel stand, 13 copper tube, 14 conical flask, 15 silicone tube, 16 wide-mouthed bottle, 17 gas washing bottle, 18 water/ice condenser, 19 U-tube, 20 stand, 21 gas flowmeter, 22 gas analyzer and 23 vent

Gas analysis

The gas products were sampled into the online gas analyzers for determining gas concentrations by a multi-component Fourier transform infrared (FTIR) gas analyzer GASMET DX-4000 for analyzing major non-hydrocarbon gases (CO and CO_2), and C_1–C_4 hydrocarbons, and an MRU-Vario Plus industrial portable flue gas analyzer for analyzing H_2 and CO_2. As a kind of syngas, the heating value of non-condensable gases is the sum of heating value of effective gas components.

Results and discussion

Characteristics analysis of shale ash

The nitrogen adsorption/desorption isotherms and pore size distributions of shale ash samples with different particle sizes are shown in Fig. 2. It can be seen from Fig. 2a–c that these isotherms of shale ash with three particle sizes belong to type II curves according to Informational Union of Pure and Applied Chemistry (IUPAC) classification method. The amount of adsorption increases slowly with the ratio of P/P_0 rising when the ratio of P/P_0 is below 0.8, but obviously improves with the ratio of P/P_0 rising when the ratio of P/P_0 is larger than 0.8. The adsorption is unsaturated at a pressure approach to the saturated vapor pressure, which indicates the capillary condensation occurs in the sample during the adsorption process of N_2. In addition, the adsorption isotherm and desorption isotherm begin to separate at about medium pressure in the adsorption isotherms of nitrogen of three shale ash samples, and the procedure of desorption falls behind that of adsorption. Thus, there appear hysteresis loops which are not typical according to five types of hysteresis loops designated as A–E by De Boer. It indicates that these particles have uniform porous structure with multi-sized pores, whose hysteresis loops are superposition of a variety of standard loops [47].

The pore structure parameters and the internal pore size distribution of shale ashes with different particle sizes are shown in Table 2 and Fig. 2d, respectively. The surface area is determined by the linear regressing calculation of the adsorption data within the P/P_0 range from 0.05 to 0.25 using BET method. Simultaneously, the pore size distribution curves are obtained from the nitrogen desorption branches by the BJH method. The surface area and pore volume of 1.25 mm shale ash are close to those of 0.60 mm shale ash. But 0.20 mm shale ash has the largest surface area of 3.928 m^2 g^{-1} and largest pore volume of 0.01348 cm^3 g^{-1}, respectively, indicating that it has the most developed pore structure among three shale ashes investigated. According to the IUPAC standard, pores can be divided into three types based on their pore sizes. Macropore is larger than 50 nm, mesopore is between 2 and 50 nm, and the micropore is smaller than 2 nm [48, 49]. As shown in Fig. 2d, the shale ash samples compose mainly of mespores with a small amount of macropores and micropores.
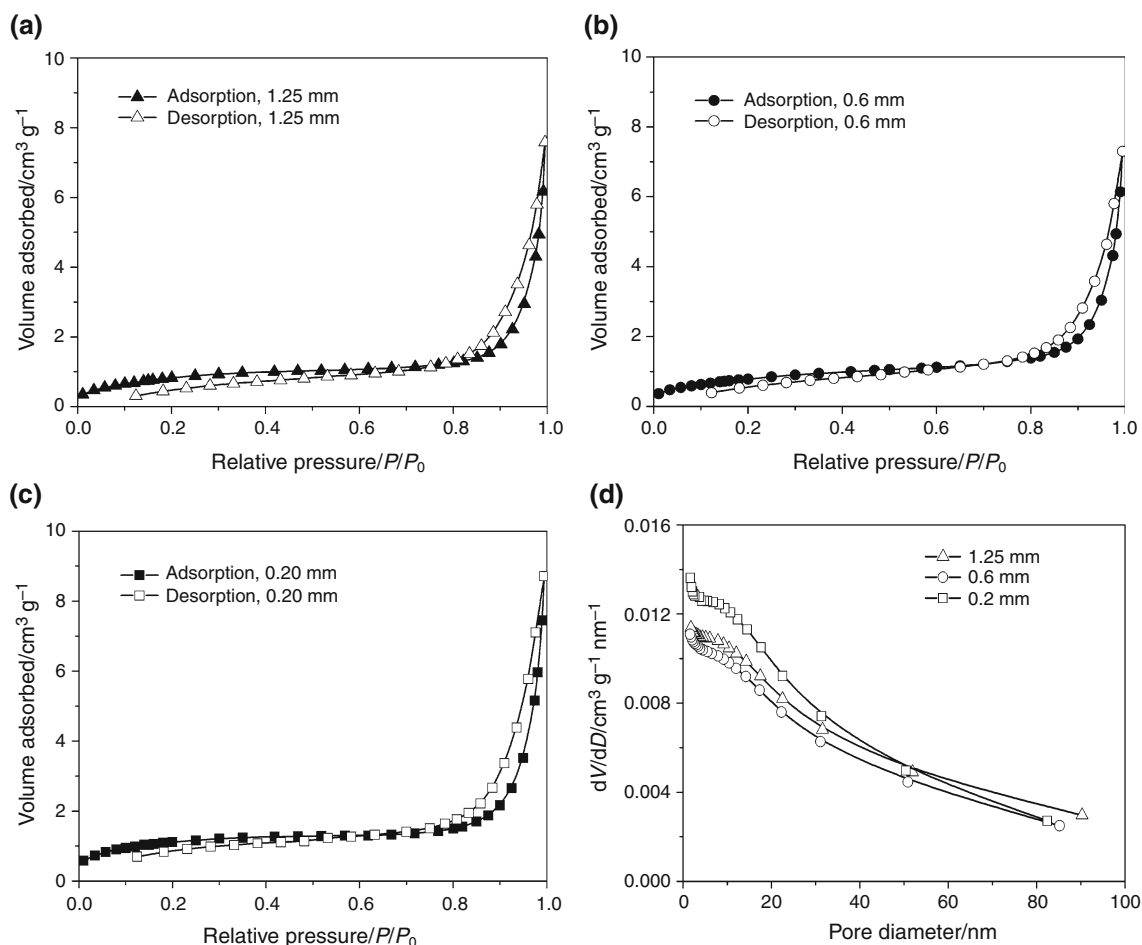
Fig. 2 Nitrogen adsorption/desorption isotherms and the pore size distributions for shale ash samples with different particle sizes. **a** 1.25 mm, **b** 0.60 mm, **c** 0.20 mm and **d** pore size distribution

Table 2 Pore structure parameters of shale ashes with different particle sizes

Test items	1.25 mm	0.60 mm	0.20 mm
BET specific surface area/m^2 g^{-1}	3.112	2.922	3.928
Pore volume/cm^3 g^{-1}	0.01172	0.01129	0.01348

The XRD diffractogram of shale ash is shown in Fig. 3. Figure 3 indicates that the mineral matters in the shale ash are mainly composed of quartz, clay minerals, calcium sulfate, different types of carbonate (aragonite, calcium carbonate and dolomite), CaO and Fe$_2$O$_3$. In addition, there are a small amount of silicate minerals, Na$_2$O, FeO and MgO and other alkali metal oxides. These components indicate that the added shale ash contains large amounts of acidic oxides, alkaline oxides and neutral oxides. Furthermore, it can be seen from the above analysis, the shale ash is porous due to being produced by high-temperature combustion. All of these chemical and physical properties
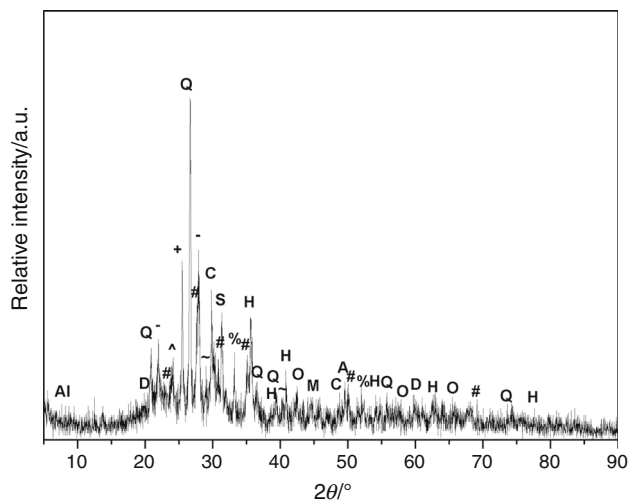

Fig. 3 XRD diffractogram of shale ash. Q, quartz; −, calcium feldspar; +, anhydrite; C, calcium carbonate; S, calcium sulfate; #, albit; ∼, calcium sulfite; H, Hematite; ^, calcium oxide; %, calcium silicate; O, orthoclase; M, magnesite; A, aluminum silicate; D, dolomite; Al, alumina

of shale ash suggest that it exhibits good adsorption capacity [36, 50]. In addition, the alkali and alkaline earth metal carbonates in shale ash are supposed to promote the conversion of organic matter in oil shale to volatile matter and increase the overall conversion rate of organic matter. The alkali and alkaline earth metal cations are well-known catalysts for pyrolysis reactions of coal and oil shale. During the pyrolysis of oil shale, these metal cations can easily react with –COOH and –OH functional groups in oil shale to form alkali-oxygen surface clusters and alkaline-oxygen surface complexes or clusters after they are mixed with the oil shale mechanically. These complexes probably serve as the active sites on the oil shale surface, resulting in significant increase in the reactivity of oil shale pyrolysis, and then increasing the conversion rate of kerogen in the oil shale [18, 51]. Karabakan and Yürüm [18] have demonstrated that pyrolysis reactions were catalyzed by alkaline earth metal cations in carbonates and inhibited by silicates. The inhibition effect of silicates seemed to be greater than the catalytic effect of the carbonates in the pyrolysis reactions of oil shale [33]. Lu et al. [52] suggested that carbonate and aluminosilicate minerals decreased the oil yield in favor of gas products during the pyrolysis of oil shale. The quartz and calcite in the mineral matters had no significant influence on the production of oils, but the acid clay minerals could easily absorb polars in oils to promote the condensation of neutral hydrocarbons in oils and thus change the products yield. Taulbee and Seibert [53] have studied the effect of organic/inorganic interactions during the pyrolysis of kerogen. The results indicated that the acid clays played important roles on the coking reactions of pyrolysis products. The more acid clays were be generally the most catalytically active [54, 55]. In addition, Torels et al. [56] have suggested that transition metals have been used in coal liquefaction as catalysts for hydrodesulfurization, deoxygenation and dehydrogenation as well as for olefin saturation to equivalent paraffins and breaking of long-chain molecules. The transition metal crystallites in the oil shale matrix offered a catalytic influence on kerogen decomposition when this occurred in the presence of hydrogen. Williams and Chishti [28, 29] believed that the shale ash or Ni–Mo/γ-Al$_2$O$_3$ catalyst has a significant catalytic effect on the secondary reactions of the generated oil vapors. Carter et al. [40, 41] also presented that the shale ash had the greatest influence on the coking reactions of oil vapors compared with shale char and gasified shale, especially certain types of clay minerals in the shale ash [42]. After adding shale ash, there were a significant decrease in the average molecular weight and an increase in the aromaticity of the shale oil [40, 41]. Therefore, the addition of the shale ash may exhibit certain catalytic effect on the pyrolysis of oil shale and then will affect the yield distribution and properties of the products.

Products yield

The processes of converting solid kerogen into liquid hydrocarbons and gas by retorting may be conceptually divided into four stages [53]: (1) thermal decomposition of the kerogen to form liquid, gas and solid char products; (2) the migration and interaction of liquid and gas products within the mineral matrix; (3) the expulsion of the products from the mineral matrix and further reactions with the surfaces of the mineral matrix and reactor walls; and (4) coalescence and condensation of the products, which are somewhat unstable and thus subject to further reactions. The first two stages occurring inside the particles are not largely affected by pyrolysis conditions except the shale particle size. The second two stages involve reactions that occur outside of the particle involving interactions between pyrolysis products as well as interactions between them and the reactor walls, particle exteriors as well as condensation train. These latter reactions are subject to limited impact by the pyrolysis conditions. Adding shale ash may affect the four reaction processes due to its chemical adsorption and catalytic properties. After adding the shale ash with smaller particle size than that of oil shale samples, they will fill a portion of pores between the oil shale particles, resulting in a reduction in the void volume and smaller average particle size of the oil shale sample. As a result, the oil shale sample is heated more rapidly and more uniformly. In addition, the shale ash exhibits catalytic effect on the oil shale pyrolysis. So the first reaction process after adding shale ash carries out more completely. And then the volatile products diffuse from reaction sites to the external surface of the oil shale particles during the second reaction stage. The interactions between volatile products inside the oil shale particles become more intense under complete heating conditions. After the volatile products escape from the oil shale particles, the secondary cracking reactions of oil vapors may occur when they emerge at high temperatures. In addition, as the mass transfer resistance of pyrolysis products increases after adding the shale ash, the more oil vapors are retained on the surface of oil shale and shale ash and then may undergo secondary coking reactions. When the volatile products diffuse out of the sample layer, there are possibly reactions occurring between the oil vapors and high-temperature reactor wall or between the components of oil vapors. So the yield distribution of pyrolysis products after adding the shale ash is determined by the integrated effects of four-step reactions.

Figure 4 indicates the yields of shale char, shale oil, non-condensable gases and water produced by retorting oil shale in the absence and presence of shale ash. It can be seen from Fig. 4 the shale char yield slightly decreases
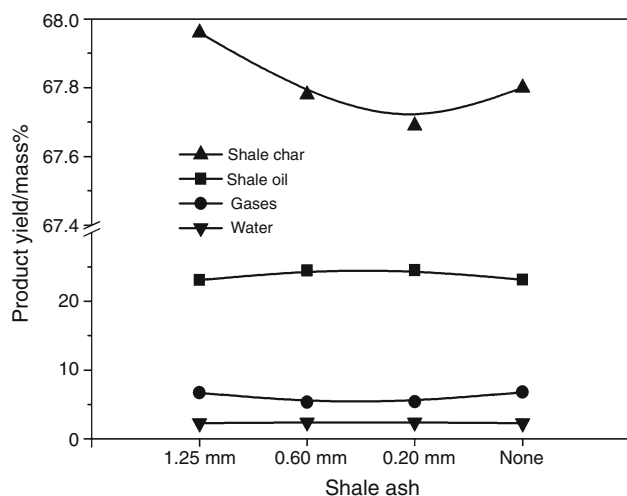
Fig. 4 Influence of shale ashes with different particle sizes on the yield of products derived by retorting oil shale

from 67.96 to 67.69 mass% with the particle size of shale ash decreasing from 1.25 to 0.20 mm, but the total yield of volatile products increases. The shale oil yield after adding 1.25 mm, 0.60 mm and 0.20 mm shale ashes is 23.15 mass%, 24.49 mass% and 24.52 mass%, respectively, which is 99.70%, 1.058 and 1.059 times that obtained in the absence of shale ash. The results indicate that the shale oil yield increases after adding 0.6 mm and 0.2 mm shale ashes compared with that obtained without adding shale ash, especially 0.2 mm, but it increases after adding 1.25 mm shale ash. It is possibly because adding shale ash not only improves the kerogen pyrolysis, but also enhances the secondary reactions of oil vapors. There are more abundant active sites in the surface of shale ash with smaller particle size, which has higher catalytic activity for the kerogen pyrolysis. In addition, adding the shale ash with smaller particle size reduces the average diameter of the mixture of oil shale and shale ash, which is helpful for accelerating heating of the kerogen to obtain more uniform temperature distribution, and then achieving more complete pyrolysis of the kerogen. However, the heating effect of kerogen becomes worse in the presence of shale ash with larger particle size, and more high-temperature pores appear between the oil shale and the shale ash particles. The high-temperature cracking reactions are more likely to occur when the oil vapors escape from surface of oil shale particles. Therefore, the shale oil yield increases and reaches the maximum after adding 0.2 mm shale ash, but it decreases and reaches the minimum after adding 1.25 mm shale ash.

The non-condensable gases yield after adding 1.25 mm, 0.60 mm and 0.20 mm shale ashes is 6.7 mass%, 5.34 mass% and 5.4 mass%, respectively, which is 98.67%, 78.65% and 79.53% of that obtained in the

absence of shale ash. The results indicate that the non-condensable gases yield decreases after adding the shale ash compared with that obtained without adding shale ash and declines with reducing the particle size of shale ash. It may be attributed to that the mineral matters contained in the shale ash have catalytic effects on the oil shale pyrolysis and the secondary reactions of the oil vapors [52, 53]. In addition, the kerogen pyrolysis is promoted after the shale ash fills the pores between the oil shale particles, and the oil vapors are more easily adsorbed on the surface of the oil shale and shale ash to undergo coking reactions due to the higher mass transfer resistance. And the secondary reactions occur more easily when the oil vapors escape from the sample layer. As the particle size of shale ash decreases and its specific surface area increases, the kerogen pyrolysis becomes more completely, but the secondary reactions of the oil vapors also get more intense. Taulbee and Seibert [53] have reported that the addition and dehydrogenation reactions of more gas components take place to form monocyclic aromatic hydrocarbons in the presence of mineral matrices [57, 58]. Therefore, the yield of non-condensable gases decreases after adding the shale ash with three particle sizes, especially 0.60 mm.

Concentration distribution of non-condensable gases

The non-condensable gases generated from retorting oil shale mainly comprise some non-hydrocarbon gases (CO_2, CO and H_2) and other small molecule hydrocarbon gases (C_1–C_4 alkanes and C_2–C_4 alkenes). The volume percentage of these non-condensable gases obtained in the absence and presence of the shale ash in relation to reaction time is shown in Fig. 5. It can be seen from Fig. 5 that the volume percentages of CO_2, CH_4 and H_2 are larger, while those of CO and C_2–C_4 hydrocarbons are lower. Adding the shale ash shortens the heating time to reach their peak concentrations for all the gases and makes the peak concentrations shift to the lower temperatures. It is possibly because shale ash contains a large amount of catalysts, such as clay minerals, which are helpful for reducing the activation energy of the pyrolysis reactions, increasing the reaction rate and then affecting the reaction mechanism [59]. Therefore, the addition of shale ash is beneficial for promoting the pyrolysis reactions of oil shale and the secondary reactions of the oil vapors, resulting in the peak concentration of each gas shifting to the lower reaction temperature. In addition, there are inconsistent change trends in the peak concentrations of all the gases after adding shale ashes. The addition of shale ashes with different particle sizes has inconsistent effects on the peak concentration and evolution temperature range of different gases. There is only one major peak concentration for H_2
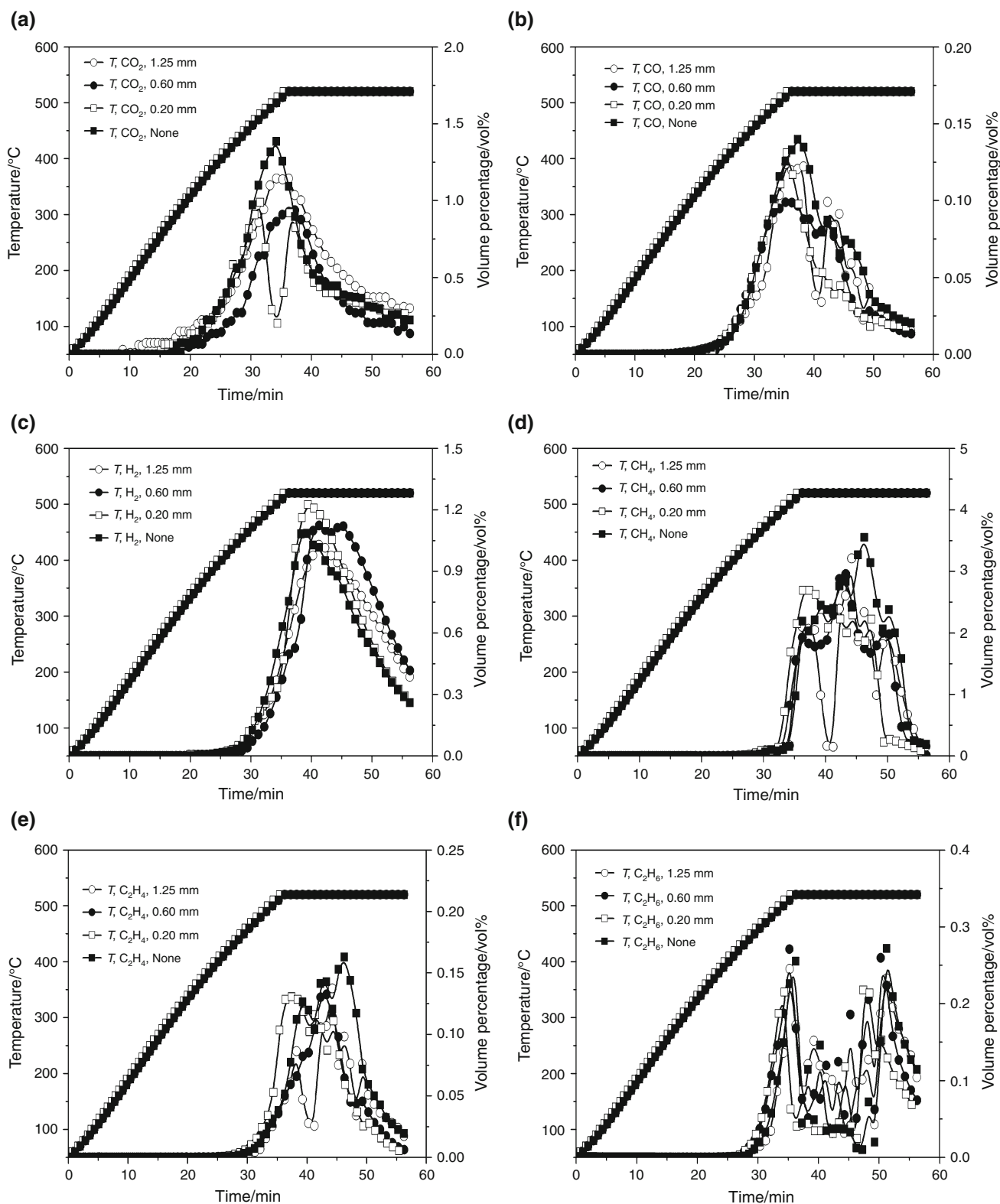
Fig. 5 Volume percentage of non-condensable gases obtained from retorting oil shale in the presence of shale ashes with different particle sizes as a function of reaction time. **a** CO_2, **b** CO, **c** H_2, **d** CH_4, **e** C_2H_4, **f** C_2H_6, **g** C_3H_6, **h** C_3H_8, **i** C_4H_8 and **j** C_4H_{10}
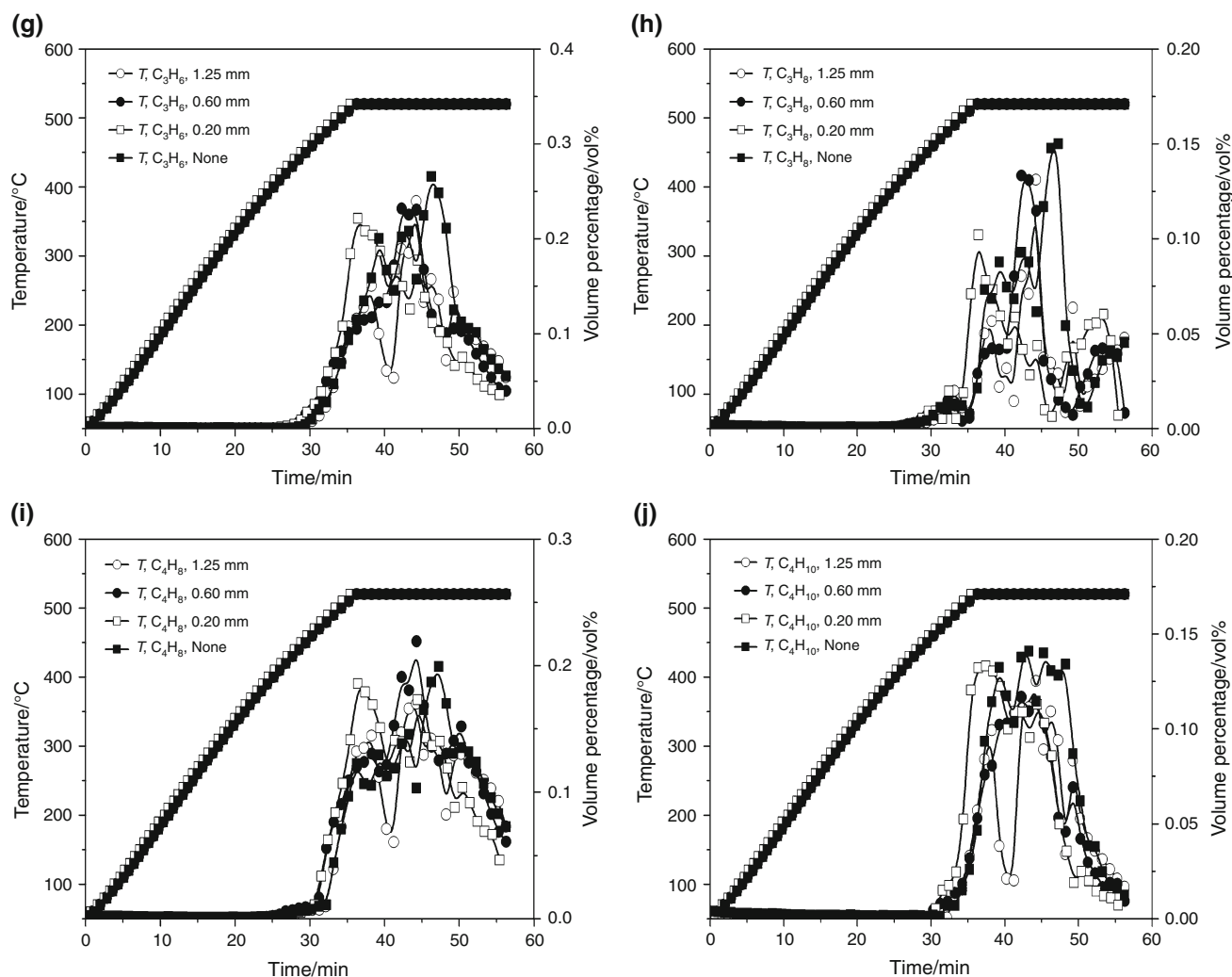
Fig. 5 continued

during the pyrolysis process before and after the addition of shale ashes. And there is only one major peak concentration for both CO and CO_2 in the pyrolysis process before adding shale ashes, but two peak concentrations appear for them after adding 1.25 mm and 0.20 mm shale ashes. Other hydrocarbon gases have two major peak concentrations before and after the addition of shale ashes. Adding shale ash increases the maximum peak concentration of C_4H_8 and H_2, especially H_2, but decreases those of other gases. This may be because that the pyrolysis of kerogen and the decomposition of bitumen have become more intense after the addition of shale ashes, so the amount of H_2 generated increases. Meanwhile, adding the shale ash may promote the dehydrogenation of side chains attached to aromatic hydrocarbons, cyclization and dehydrogenation of aliphatic hydrocarbons, and the addition and subsequent dehydrogenation of gas components due to the catalytic properties of shale ashes [11, 53], so the concentration of H_2 increases after the addition of shale ashes.

Mass distribution and heating value of non-condensable gases

The mass distribution of non-condensable gases is calculated by the volume percentage shown in Fig. 5 and volume flow rate of the gases. The heating value of non-condensable gases is the sum of low heating value of effective gas components. The mass distribution and heating value of non-condensable gas produced in the absence and presence of the shale ash are indicated in Fig. 6. As can be seen from Fig. 6, the non-condensable gases mainly contain CO_2 and CH_4, the yields of which range from 1.83 to 2.90 mass% and from 1.59 to 2.10 mass%, respectively. In addition, there are also relatively small amounts of other gases, each of which has the yield of less than 0.5 mass%. The addition of shale ashes reduces the yields of several gases except CO_2, H_2, C_2H_6 and C_4H_8 compared with those obtained without adding shale ash. Adding the shale ash with three particle sizes
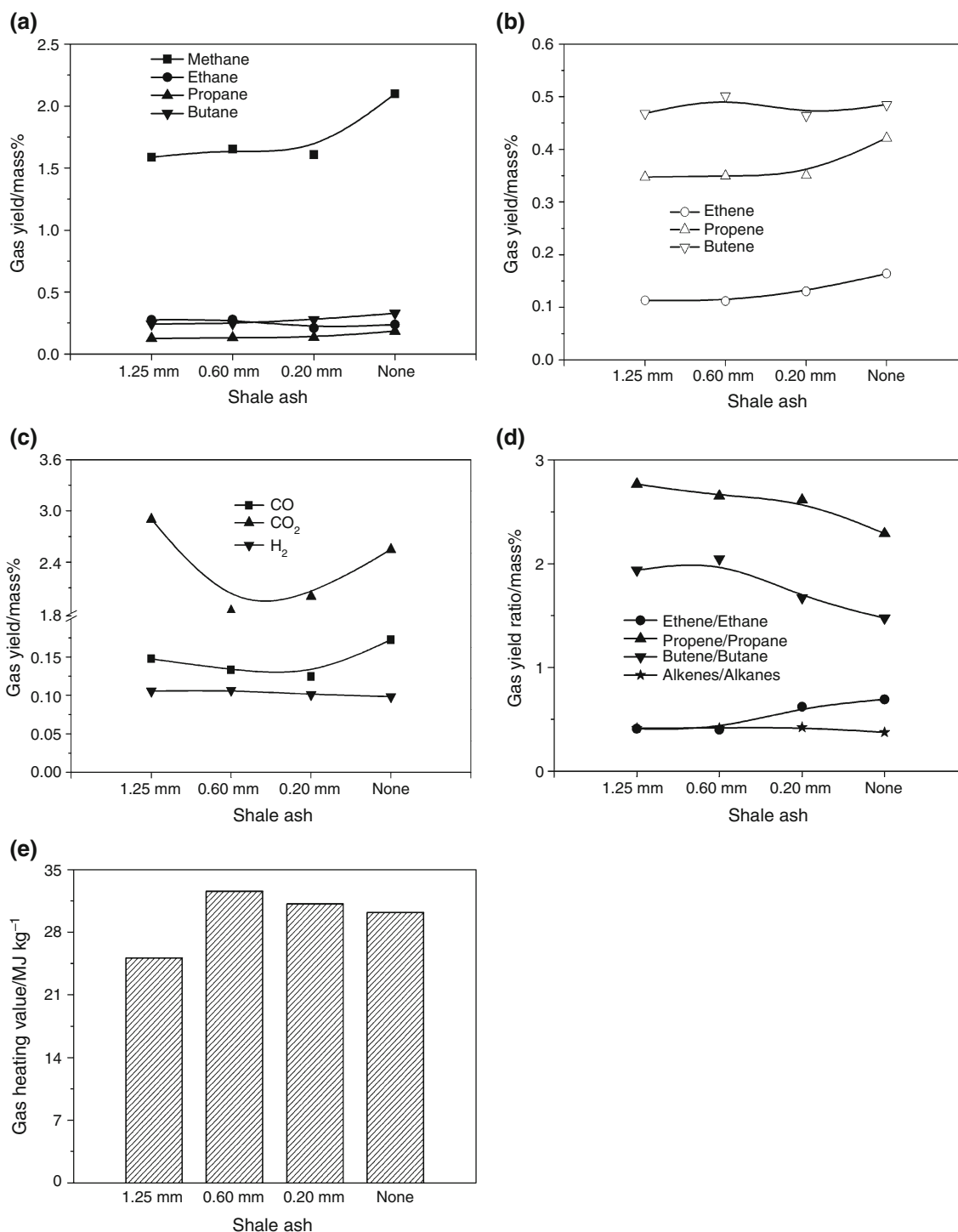
Fig. 6 Influence of shale ashes with different particle sizes on the composition and heating value of non-condensable gases. **a** Alkane gases, **b** alkene gases, **c** non-hydrocarbon gases, **d** alkene/alkane ratios and **e** heating value of non-condensable gases

increases the H_2 content, but causes different effects on the contents of CO_2, C_2H_6 and C_4H_8. The yield of CO_2 decreases when 0.20 mm and 0.60 mm shale ashes are added, whereas it increases as 1.25 mm shale ash is added. The production of C_2H_6 decreases when 0.20 mm shale ash is added, but increases when 1.25 mm and 0.60 mm shale

ashes are added. And the yield of C_4H_8 decreases in the presence of 0.20 mm and 1.25 mm shale ashes, but increases in the presence of 0.60 mm shale ash.

In addition, it is further found from Fig. 5 that the content of H_2 and the total content of C_1–C_4 alkanes decrease as the specific surface area of the shale ash

increases, while the total content of C_2–C_4 alkenes firstly decreases and then increases. And the content of CO improves as the particle size of shale ash increases. The content of CO_2 reaches maximum after adding 1.25 mm shale ash and reaches minimum after adding 0.60 mm shale ash. Adding 1.25 mm shale ash makes the contents of H_2, CO and CO_2 and the total content of C_1–C_4 alkanes higher than those obtained after adding 0.20 mm shale ash, while causes the total content of C_2–C_4 alkenes smaller. This may be because there is the larger porosity between the shale ash and oil shale after adding the shale ash with larger particle sizes, which reduces the mass transfer resistance of pyrolysis products diffusing out of the sample layer, so the amount of pyrolysis products adsorbing on the sample declines, and more bitumen and macromolecular hydrocarbons travel out of the sample layer to high-temperature environment, resulting in the thermal decomposition and gas-phase cracking reactions to generate low molecular weight gases. The gas-phase cracking reactions are dominant in the presence of the shale ash with larger particle sizes. But the bitumen and macromolecular hydrocarbons are easily adsorbed on the sample due to larger mass transfer resistance in the presence of shale ash with smaller particle size, resulting in more intense coking reactions. The remaining bitumen and macromolecular hydrocarbons will further undergo gas-phase cracking reaction after escaping from the sample layer. In addition, oil shale pyrolysis performs more completely in the presence of shale ash with smaller particle size, which produces more bitumen and macromolecular hydrocarbons as well as other gases. The peak concentrations of non-condensable gases after adding shale ash with three particle sizes are decided by the combined effects of oil shale pyrolysis and secondary reaction of macromolecular products. Adding 1.25 mm shale ash produces the more total content of C_1–C_4 alkanes and the lower total content of C_2–C_4 alkenes than those obtained in the presence of 0.20 mm shale ash. It is possibly because alkenes have larger coking reaction rate than alkanes and are more prone to undergo cyclization and dehydrogenation reactions to form coke. Moreover, the coking reaction of alkenes is more intense in the presence of silicate minerals. Alkenes can be selectively removed compared with alkanes [42].

In addition, Fig. 6 also shows the ethene/ethane, propene/propane, butene/butane and total alkene/alkane ratios in the absence and presence of shale ash. The alkene/alkane ratio has been used to determine the reaction mechanism and characterize the pyrolysis conditions. For example, Williams and Nazzal [60] and Williams and Ahmad [61] have suggested that the increase in the ethene/ethane, propene/propane, butene/butane and total alkene/alkane ratios with improving pyrolysis temperature might be related to the acceleration of the gas-phase cracking reaction [10]. As can be seen from Fig. 6, the ethene/ethane, propene/propane, butene/butane and total alkene/alkane ratios are 0.69, 2.29, 1.48 and 0.38, respectively, in the absence of shale ash. After the shale ash is added, the ethene/ethane ratio decreases and the other alkene/alkane ratios increase, which indicates that the addition of shale ash has a great influence on the structure change in the oil shale and the secondary reactions of pyrolysis products in the pyrolysis process. In addition, as the particle size of shale ash increases from 0.2 to 1.25 mm, the propene/propane ratio increases from 2.61 to 2.77, but the total alkene/alkane ratio reduces from 0.424 to 0.416. The ethene/ethane and butene/butane ratios are related to the surface area of shale ash. As the surface area increases, the ethene/ethane ratio increases from 0.40 to 0.62, but the butene/butane ratio declines from 2.05 to 1.67. Williams and Ahmad [61] have shown that the alkene/alkane ratios, especially the ethene/ethane ratio, were used as indicator of oil vapors cracking reactions. The higher alkene/alkane gases ratio was related to increased secondary gas-phase cracking reactions, while the lower alkene/alkane gases ratio might be related to secondary coking reactions [10]. Raley [62] has presented a chemical reaction mechanism to explain the oil vapor cracking reactions and found that the declined oil yield was related to the increased ethene/ethane ratio. The propene/propane ratio behaved similarly. Several kinds of alkene/alkane ratios exhibit different change trends after the addition of shale ash. It is possibly because the cracking reactions and coking reactions of oil vapors after the addition of shale ash simultaneously occur, which demonstrates different impacts on these alkene/alkane ratios.

It can also be seen from Fig. 6e that after adding 0.20 mm, 0.60 mm and 1.25 mm shale ashes, the heating values of non-condensable gases are 31.180 and 32.576 and 25.115 MJ kg^{-1}, respectively, and it is 30.209 MJ kg^{-1} without adding shale ash. This shows that adding shale ashes with smaller particle sizes are more conducive to obtain non-condensable gases of higher heating value. In addition, 0.20 mm shale ash produces the largest shale oil yield. So the addition of 0.20 mm shale ash is the optimal for improving the shale oil and the conversion rate of kerogen to volatile products.

Conclusions

In this paper, the gas evolution characteristics were investigated in the absence and presence of shale ash with different particle sizes. Based on the results obtained, the following conclusions are drawn:

1. The shale ash samples compose mainly of mespores with a small amount of macropores and micropores and contain large amounts of acidic oxides, alkaline oxides and neutral oxides. 1.25 mm and 0.60 mm shale ashes have similar pore structures, while 0.20 mm shale ash has the most developed pore structure with the largest surface area of 3.928 m^2 g^{-1} and largest pore volume of 0.01348 cm^3 g^{-1}. The chemical and physical properties of shale ashes suggest that they have good adsorption capacity and certain catalytic performance. The addition of shale ash may affect oil shale retorting, resulting in the change in the yield distribution and characteristics of pyrolysis products.

2. There are slight decrease in the shale char yield and increase in the total yield of volatile products with the particle size of shale ash decreasing from 1.25 to 0.20 mm. The oil yields increase after adding 0.20 mm and 0.60 mm shale ashes compared with that obtained without adding shale ash, especially 0.20 mm, while reduce after the addition of 1.25 mm shale ash. In addition, the non-condensable gases yield decreases after adding shale ashes with three particle sizes, especially 0.60 mm.

3. The volume percentages of CO_2, CH_4 and H_2 in the non-condensable gases produced are much larger, and those of CO and C_2–C_4 hydrocarbons are lower in the absence and presence of shale ashes. Adding the shale ash makes the peak concentrations of all the gases shift to the lower temperatures. Adding shale ashes with different particle sizes have inconsistent effects on the peak numbers, the value of peak concentration and the corresponding evolution temperature range of each gas. In addition, adding shale ash increases the maximum peak concentrations of C_4H_8 and H_2, especially H_2, but decreases those of other gases.

4. The produced non-condensable gases mainly contain CO_2 and CH_4, and smaller amounts of other gases in terms of their mass distribution in the absence and presence of shale ashes. The addition of shale ashes reduces the yields of several gases except CO_2, H_2, C_2H_6 and C_4H_8 compared with those obtained without adding shale ash. Adding the shale ash with three particle sizes increases the H_2 content, but causes different effects on the contents of CO_2, C_2H_6 and C_4H_8. As the specific surface area of the shale ash increases, the content of H_2 and the total content of C_1–C_4 alkanes decrease, while the total content of C_2–C_4 alkenes firstly decreases and then increases. And the content of CO improves as the particle size of shale ash increases. The content of CO_2 reaches maximum after adding 1.25 mm shale ash and reaches minimum after adding 0.60 mm shale ash. Adding 1.25 mm shale ash slightly increases the contents of H_2, CO and CO_2 and

the total content of C_1–C_4 alkanes, but decreases the total content of C_2–C_4 alkenes compared with those obtained after adding 0.20 mm shale ash.

5. Adding the shale ash decreases the ethene/ethane ratio and increases the other alkene/alkane ratios compared with those obtained without adding shale ash. The propene/propane ratio increases as the particle size of shale ash increases from 0.2 mm to 1.25 mm, and 0.2 mm shale ash among the three shale ash samples also produces the lowest ethene/ethane ratio, which indicate there are the most significant coking reactions in the presence of 0.2 mm shale ash. In addition, adding shale ashes with smaller particle sizes are more conducive to obtain non-condensable gases of high heating value. The addition of 0.20 mm shale ash is the optimal for improving the shale oil and the conversion rate of kerogen to volatile products.

References

1. Dyni JR. Geology and resources of some world oil-shale deposits. Oil Shale. 2003;20(3):193–252.
2. Liu QQ, Han XX, Li QY, Huang YR, Jiang XM. TG–DSC analysis of pyrolysis process of two Chinese oil shales. J Therm Anal Calorim. 2014;116:511–7.
3. Tiwari P, Deo M. Compositional and kinetic analysis of oil shale pyrolysis using TGA–MS. Fuel. 2012;94:333–41.
4. Na JG, Im CH, Chung SH, Lee KB. Effect of oil shale retorting temperature on shale oil yield and properties. Fuel. 2012;95:131–5.
5. Dung NV. Factors affecting product yields and oil quality during retorting of Stuart oil shale with recycled shale: a screening study. Fuel. 1995;74:623–7.
6. Al-Harahsheh A, Al-Ayed O, Al-Harahsheh M, Abu-El-Halawah R. Heating rate effect on fractional yield and composition of oil retorted from El-lajjun oil shale. J Anal Appl Pyrol. 2010;89:239–43.
7. Maaten B, Loo L, Konist A, Siirde A. Mineral matter effect on the decomposition of Ca-rich oil shale. J Therm Anal Calorim. 2018;131:2087–91.
8. Li MY, Zhan JH, Lai DG, Tian Y, Liu XX, Xu GW. Study on the evolution characteristic of intermediate during the pyrolysis of oil shale. J Therm Anal Calorim. 2017;130:2227–38.
9. Wang S, Song LZ, Jiang XM. Prediction of gaseous products from Dachengzi oil shale pyrolysis through combined kinetic and thermodynamic simulations. J Therm Anal Calorim. 2018;134:1129–44.
10. Campbell JH, Kokinas GJ, Gallegos G, Gregg M. Gas evolution during oil shale pyrolysis. 1: nonisothermal rate measurements. Fuel. 1980;59(10):718–26.

11. Campbell JH, Gallegos G, Gregg M. Gas evolution during oil shale pyrolysis. 2. Kinetic and stoichiometric analysis. Fuel. 1980;59(10):727–32.

12. Huss EB, Burnham AK. Gas evolution during pyrolysis of various Colorado oil shales. Fuel. 1982;61(12):1188–96.

13. Marshall CP, Kannangara GSK, Wilson MA, Guerbois JP, Hartung-Kagi B, Hart G. Potential of thermogravimetric analysis coupled with mass spectrometry for the evaluation of kerogen in source rocks. Chem Geol. 2002;184(3–4):185–94.

14. Charlesworth JM. Oil shale pyrolysis. 2. Kinetics and mechanism of hydrocarbon evolution. Ind Eng Chem Process Des Dev. 1985;24(4):1125–32.

15. Wong CM, Crawford RW, Burnham AK. Determination of sulfur-containing gases from oil shale pyrolysis by triple quadrupole mass spectrometry. Anal Chem. 1984;56(3):390–5.

16. Reynolds JG, Crawford RW, Burnham AK. Analysis of oil shale and petroleum source rock pyrolysis by triple quadrupole mass spectrometry: comparisons of gas evolution at the heating rate of 10 °C/min. Energy Fuel. 1991;5(3):507–23.

17. Abbasi-Atibeh E, Yozgatligil A. A study on the effects of catalysts on pyrolysis and combustion characteristics of Turkish lignite in oxy-fuel conditions. Fuel. 2014;115:841–9.

18. Karabakan A, Yürüm Y. Effect of the mineral matrix in the reactions of oil shales: 1. Pyrolysis reactions of Turkish Göynük and US Green River oil shales. Fuel. 1998;77(12):1303–9.

19. Sadiki A, Kaminsky W, Halim H, Bekri O. Fluidised bed pyrolysis of Moroccan oil shales using the hamburg pyrolysis process. J Anal Appl Pyrol. 2003;70(2):427–35.

20. Floess JK, Plawsky J, Longwell JP, Peters WA. Effects of calcined dolomite on the fluidized bed pyrolysis of a Colorado oil shale and a Texas lignite. Ind Eng Chem Process Des Dev. 1985;24(3):730–7.

21. Ellig DL, Lai CK, Mead DW, Longwell JP, Peters WA. Pyrolysis of volatile aromatic hydrocarbons and *n*-heptane over calcium oxide and quartz. Ind Eng Chem Process Des Dev. 1985;24(4):1080–7.

22. Bakr MY, Yokono T, Sanada Y, Akiyama M. Role of pyrite during the thermal degradation of kerogen using in situ high-temperature ESR technique. Energy Fuel. 1991;5(3):441–4.

23. Gai RH, Jin LJ, Zhang JB, Wang JY, Hu HQ. Effect of inherent and additional pyrite on the pyrolysis behavior of oil shale. J Anal Appl Pyrolysis. 2014;105:342–7.

24. Hascakir B, Babadagli T, Akin S. Experimental and numerical simulation of oil recovery from oil shales by electrical heating. Energy Fuel. 2008;22(6):3976–85.

25. Hascakir B, Akin S. Recovery of turkish oil shales by electromagnetic heating and determination of the dielectric properties of oil shales by an analytical method. Energy Fuel. 2010;24(1):503–9.

26. Feng J, Xue XY, Li XH, Li WY, Guo XF, Liu K. Products analysis of Shendong long-flame coal hydropyrolysis with iron-based catalysts. Fuel Process Technol. 2015;130:96–100.

27. Jiang HF, Song LH, Cheng ZQ, Chen J, Zhang L, Zhang MY, Hu MJ, Li JN, Li JF. Influence of pyrolysis condition and transition metal salt on the product yield and characterization via Huadian oil shale pyrolysis. J Anal Appl Pyrolysis. 2015;112:230–6.

28. Williams PT, Chishti HM. Two stage pyrolysis of oil shale using a zeolite catalyst. J Anal Appl Pyrolysis. 2000;55(2):217–34.

29. Williams PT, Chishti HM. Influence of residence time and catalyst regeneration on the pyrolysis–zeolite catalysis of oil shale. J Anal Appl Pyrolysis. 2001;60(2):187–203.

30. Fan C, Yan JW, Huang YR, Han XX, Jiang XM. XRD and TG-FTIR study of the effect of mineral matrix on the pyrolysis and combustion of organic matter in shale char. Fuel. 2015;139:502–10.

31. Shi WJ, Wang Z, Song LW, Li XY. Pyrolysis of Huadian oil shale under catalysis of shale ash. J Anal Appl Pyrolysis. 2017;123:160–4.

32. Karabakan A, Yürüm Y. Effect of the mineral matrix in the reactions of shales. Part 2. Oxidation reactions of Turkish Göynük and US Western Reference oil shales. Fuel. 2000;79:785–92.

33. Yürüm Y, Kramer R, Levy M. Interaction of kerogen and mineral matrix of an oil shale in an oxidative atmosphere. Thermochim Acta. 1985;94(2):285–93.

34. Liu XS. Experiment analysis of the catalysis function of shale ash in fluidized retorting of oil shale solid heat carrier. Guang Dong Chem Ind. 2013;40(4):38–40 **(in Chinese, with English abstract)**.

35. Shi WJ, Wang Z, Duan Y, Li SG, Song WL. Influence of shale ash on pyrolytic behaviors of oil shale. Chin J Process Eng. 2015;15(2):266–71 **(in Chinese, with English abstract)**.

36. Oja V, Elenurm A, Rohtla I, Tali E, Tearo E, Yanchilin A. Comparison of oil shales from different deposits: oil shale pyrolysis and co-pyrolysis with ash. Oil Shale. 2007;24(2):101–8.

37. Niu MT, Wang S, Han XX, Jiang XM. Yield and characteristics of shale oil from the retorting of oil shale and fine oil-shale ash. Appl Energy. 2013;111:234–9.

38. Huang L, Zhang YM, Zhang L, Zhang XC, Sun GG. Effects of shale ash and FCC catalysts on adjusting secondary reactions of volatiles in oil shale pyrolysis. CIESC J. 2017;68(10):3770–8 **(in Chinese, with English abstract)**.

39. Dung NV. Pyrolysis of Stuart oil shale in the presence of recycled shale. Fuel. 1990;69(4):497–501.

40. Carter SD, Taulbee DN, Robl TL. The relative coke-inducing tendencies of pyrolysed, gasified and combusted Devonian oil shales. Fuel. 1993;72(6):851–4.

41. Carter SD, Citiroglu M, Gallacher J, Snape CE, Mitchell S, Lafferty CJ. Secondary coking and cracking of shale oil vapours from pyrolysis or hydropyrolysis of a Kentucky Cleveland oil shale in a two-stage reactor. Fuel. 1994;73(9):1455–8.

42. Ballice L. Effect of demineralization on yield and composition of the volatile products evolved from temperature-programmed pyrolysis of Beypazari (Turkey) oil shale. Fuel Process Technol. 2005;86(6):673–90.

43. Han XX, Jiang XM, Cui ZG. Studies of the effect of retorting factors on the yield of shale oil for a new comprehensive utilization technology of oil shale. Appl Energy. 2009;86(11):2381–5.

44. Wang S, Jiang XM, Han XX, Tong JH. Effect of retorting temperature on product yield and characteristics of non-condensable gases and shale oil obtained by retorting Huadian oil shales. Fuel Process Technol. 2014;121(1):9–15.

45. Wang S, Wang Q, Jiang XM, Han XX, Ji HS. Compositional analysis of bio-oil derived from pyrolysis of seaweed. Energy Convers Manag. 2013;68:273–80.

46. Włodarzyk-Stasiak M, Jamroz J. Specific surface area and porosity of starch extrudates determined from nitrogen adsorption date. J Food Eng. 2009;93:379–85.

47. Yan JM, Zhang QY, Gao JZ. Adsorption and agglomeration. Beijing: Science & Technology Press; 1979. p. 118–23.

48. Zdravkov BD, Čermák JJ, Šefara M, Janků J. Pore classification in the characterization of porous materials: a perspective. Cent Eur J Chem. 2007;5(2):383–95.

49. Donohue MD, Aranovich GL. Adsorption hysteresis in porous solids. J Colloid Interface Sci. 1998;205(1):121–30.

50. Al-Qodah Z. Adsorption of dyes using shale oil ash. Water Res. 2000;34(17):4295–303.

51. Joseph JT, Forrai TR. Effect of exchangeable cations on liquefaction of low rank coals. Fuel. 1992;71(1):75–80.

52. Lu ST, Ruth E, Kaplan IR. Pyrolysis of kerogens in the absence and presence of montmorillonite-I. The generation, degradation

and isomerization of steranes and triterpanes at 200 and 300 °C. Org Geochem. 1989;14(5):491–9.

53. Taulbee DN, Seibert ED. Comparison of the hydrocarbon pyrolysis products from a Devonian type II kerogen to those from kerogen/mineral blends. Energy Fuel. 1987;1(6):514–9.

54. Dembicki H, Horsfield B, Ho TTY. Source rock evaluation by pyrolysis-gas chromatography. AAPG Bull. 1983;67(7):1094–103.

55. Horsfield B, Douglas AG. The influence of minerals on the pyrolysis of kerogens. Geochim Cosmochim Acta. 1980;44(8):1119–31.

56. Torels N, Veryklos XE, Grossmann E. Catalytic effects of transition metals on oil shale pyrolysis. Ind Eng Chem Process Des Dev. 1986;25:552–7.

57. Greenfelder BS, Voge HH, Good GM. Catalytic and thermal cracking of pure hydrocarbons: mechanisms reaction. Ind Eng Chem. 1949;41(11):2573–82.

58. Hershkowitz F, Olmstead WN, Rhodes RP, Rose KD. Molecular mechanism of oil shale pyrolysis in nitrogen and hydrogen atmospheres. Am Chem Soc Symp. 1983;28(1):301–16.

59. Johns WD. Clay minerals and petroleum-forming reactions during burial and diagenesis. AAPG Bull. 1972;56(11):2160–7.

60. Williams PT, Nazzal JM. Polycyclic aromatic compounds in shale oils: influence of process conditions. Environ Technol. 1998;19(8):775–87.

61. Williams PT, Ahmad N. Influence of process conditions on the pyrolysis of Pakistani oil shales. Fuel. 1999;78(6):653–62.

62. Raley JH. Monitoring oil shale retorts by off-gas alkene/alkane ratios. Fuel. 1980;59(6):419–24.